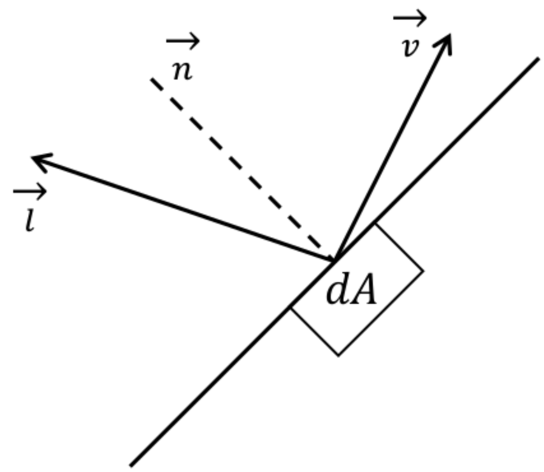

Figure 1: Geometry of photometric vision

1 Calibrated photometric stereo

1.1 Understanding n-dot-l lighting

In figure 1 above,

- n: surface normal
- l: light source vector
- v: viewing direction

n-dot-l is the product between the surface normal and the light direction both of which are normalized vectors. This the same as the cosine of angle between the two vectors. The dot product comes from the following equations: Lambertian BRDF:

$$\frac{\rho_d}{\pi} \tag{1a}$$

For angle θ_i between the source and the surface normal:

$$L = \frac{\rho_d}{\pi} I cos(\theta_i) = \frac{\rho_d}{\pi} I \vec{n}.\vec{s} \tag{1b}$$

The dot product comes from cosine of the angle between the light source vector and the surface normal. The viewing directions does not matter as the surface appears equally bright in all the directions, i.e. surface brightness is independent of the viewing angle and thus also independent of $\vec{v}$.
When an area of a surface is illuminated by a source, the irradiance on the area element

dA is directly proportional to cosine of the angle between the surface normal and the light direction. Moreover, the light is then scattered according to the aforementioned lambertian cosine law. Thus, the radiance only depends on the angle between surface normal and the light and not on the vantage point or viewing angle of the observer.

1.2 Rendering n-dot-l lighting

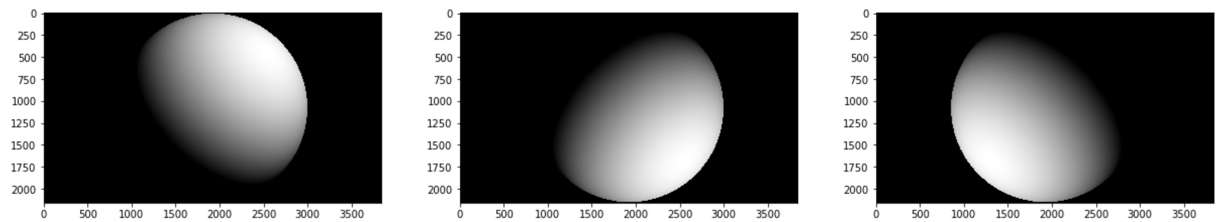

Figure 2: Rendering of the sphere with different light directions.

The Left to right in figure 2 we have the following light directions:

1. $L = \frac{(1,1,1)}{\sqrt{3}}$
2. $L = \frac{(1,-1,1)}{\sqrt{3}}$
3. $L = \frac{(-1,-1,1)}{\sqrt{3}}$

1.3 Code: Loading Data

1.4 Initials

The dimensions of L is 3 × 7 and B has dimensions 3 × P. The dimension of

$$I = L^T B \tag{2}$$

would be 7 $\times P$.

The rank of **I** should be 3 so that the normal map can be recovered accurately and efficiently.

The singular values of I are:

[79.36, 13.16, 9.22, 2.42, 1.62, 1.26, 0.89]

The singular values do not agree with the rank 3 requirement. The rank 3 structure is not observed as we have more measurements than variables, giving rise to an over-determined system.

1.5 Estimating pseudonormals

Equation in 2 can be wriiten in matrix form as:

$$\begin{bmatrix} I_1 \\ I_2 \\ I_3 \end{bmatrix} = \begin{bmatrix} s_1^T \\ s_2^T \\ s_3^T \end{bmatrix} \rho \mathbf{n} \tag{3}$$

Therefore, by comparison with $Ax = y$, matrix A would be

$$\begin{bmatrix} s_1^T \\ s_2^T \\ s_3^T \end{bmatrix} \tag{4}$$

The vector y would be all the intensities values for the luminescence channels of the input images.

1.6 Albedos and Normals

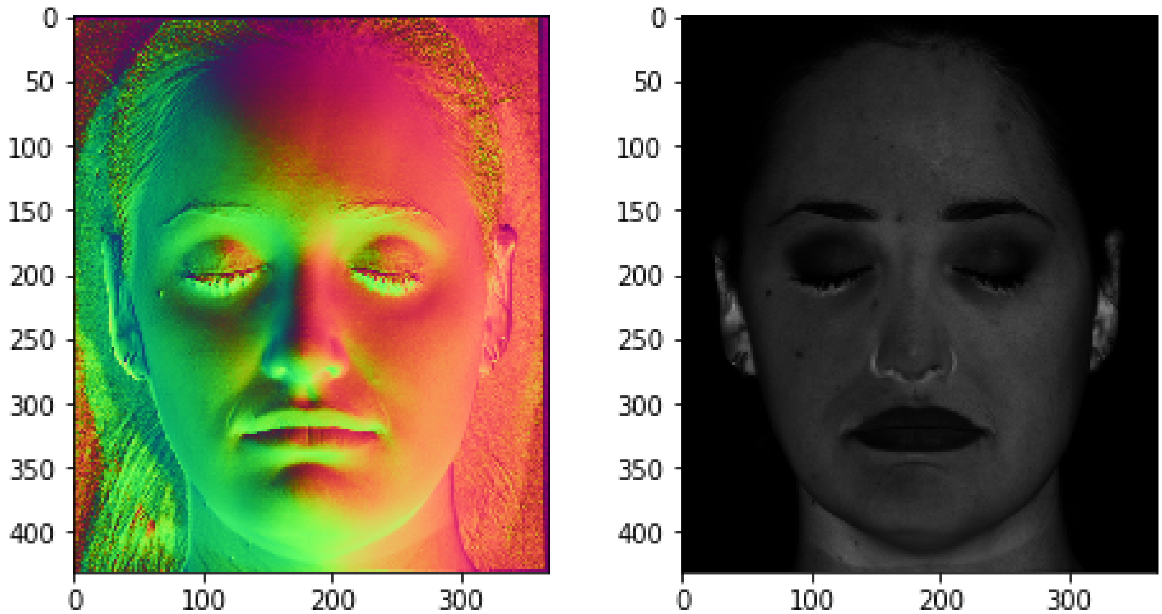

Figure 3: Rainbow map of Normal image (Left) and Gray colormap of the albedo image (right)

From the albedo image on the right, the regions under the nose and in the ears, which were originally dark, became brightest due to global inter-reflection as the light bounces back and forth multiple times. For the normal image on the left, the face looks more rounded.

1.7 Normal and depth

The surface is represented by (x,y,z), where the depth map is denoted as $z = f(x, y)$. Let the surface gradient in directions x and y be:

$$a = \frac{\delta z}{\delta x} \tag{5a}$$

$$b = \frac{\delta z}{\delta y} \tag{5b}$$

From equation above a small change δx in x reflects a change in depth as $\delta z = a\delta x$, and a similar relationship can be established for δy. Now, as a normal is perpendicular to all the tangents, and is in the direction (-a,-b,1)^T the unit normal can be shown as:

$$n = \frac{(-a, -b, 1)^T}{\sqrt{a^2 + b^2 + 1}} \tag{6}$$

Similarly, the individual normals can be computed as:

$$n_1 = \frac{(-a)^T}{\sqrt{a^2 + b^2 + 1}} \tag{7a}$$

$$n_2 = \frac{(-b)^T}{\sqrt{a^2 + b^2 + 1}} \tag{7b}$$

$$n_3 = \frac{(1)}{\sqrt{a^2 + b^2 + 1}} \tag{7c}$$

Therefore,

$$a = \frac{-n_1}{n_3} = \frac{\delta z}{\delta x} \tag{7d}$$

$$b = \frac{-n_2}{n_3} = \frac{\delta z}{\delta y} \tag{7e}$$

Thus, the normal depends on the partial derivatives.

1.8 Understanding Integrability of Gradients

$$g = \begin{bmatrix} 1 & 2 & 3 & 4 \\ 5 & 6 & 7 & 9 \\ 10 & 11 & 12 & 13 \\ 14 & 15 & 16 & 17 \end{bmatrix} \tag{8}$$

Using,
$g_x(x_i, y_j) = g(x_{i+1}, y_j) - g(x_i, y_j)$
$g_y(x_i, y_j) = g(x_i, y_{j+1}) - g(x_i, y_j)$

$$g_x = \begin{bmatrix} 1 & 1 & 1 & 1 \\ 1 & 1 & 1 & 1 \\ 1 & 1 & 1 & 1 \\ 1 & 1 & 1 & 1 \end{bmatrix} \tag{9}$$

$$g_y = \begin{bmatrix} 4 & 4 & 4 & 4 \\ 4 & 4 & 4 & 4 \\ 4 & 4 & 4 & 4 \\ 4 & 4 & 4 & 4 \end{bmatrix} \tag{10}$$

Given, $g(0, 0) = 0$,

Row 1 of reconstructed g:

$$g(1, 0) = g(0, 0) + g_x(0, 0) = 2 \tag{11a}$$
$$g(2, 0) = g(1, 0) + g_x(1, 0) = 3 \tag{11b}$$
$$g(3, 0) = g(2, 0) + g_x(2, 0) = 4 \tag{11c}$$

Column 1 of reconstructed g from g_y:

$$g(0, 1) = g(0, 0) + g_y(0, 0) = 5 \tag{12a}$$
$$g(0, 2) = g(0, 1) + g_y(0, 1) = 9 \tag{12b}$$

$$g(0,3) = g(0,2) + g_y(0,2) = 13 \tag{12c}$$

Reconstructed matrix

- Reconstructed Matrix:

$$g = \begin{bmatrix} 1 & 2 & 3 & 4 \\ 5 & 6 & 7 & 8 \\ 9 & 10 & 11 & 12 \\ 13 & 14 & 15 & 16 \end{bmatrix} \tag{13}$$

Similarly, g can be reconstructed from g_y as:

$$g(0,1) = g(0,0) + g_y(0,0) = 5 \tag{14a}$$

$$g(0.2) = g(0,1) + g_y(0,1) = 9 \tag{14b}$$

$$g(0,3) = g(0,2) + g_y(0,2) = 13 \tag{14c}$$

The remaining rows can be constructed using g_x.

$$g = \begin{bmatrix} 1 & 2 & 3 & 4 \\ 5 & 6 & 7 & 8 \\ 9 & 10 & 11 & 12 \\ 13 & 14 & 15 & 16 \end{bmatrix} \tag{15}$$

Thus, the reconstructed g is the same for both the cases.

The following modifications can be made for turning g_x and g_y non-integrable is:

1. If the gradient matrix has unequal elements, then it could result in a different g.
2. Also, if the elements of the gradient matrices are discontinuous/non-consecutive.

1.9 Shape Estimation

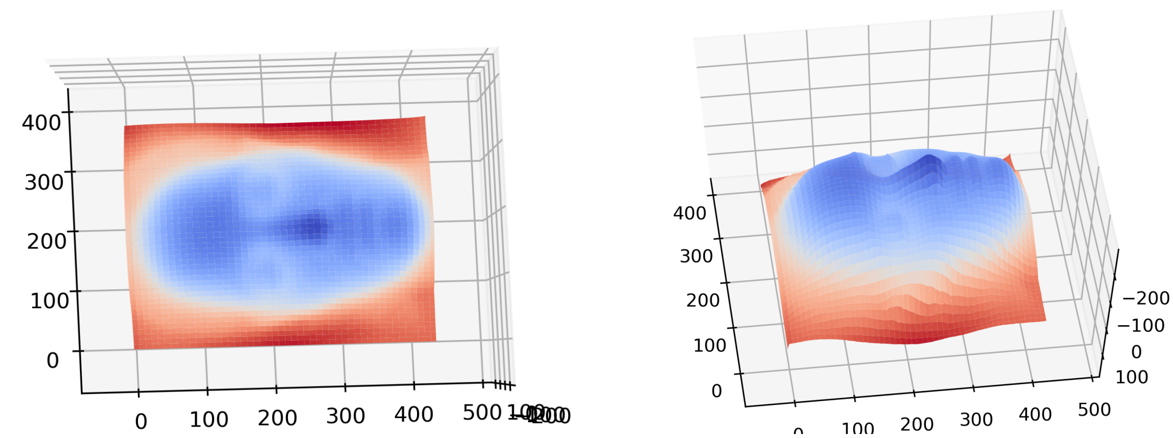

Figure 4: Depth Map from Normal

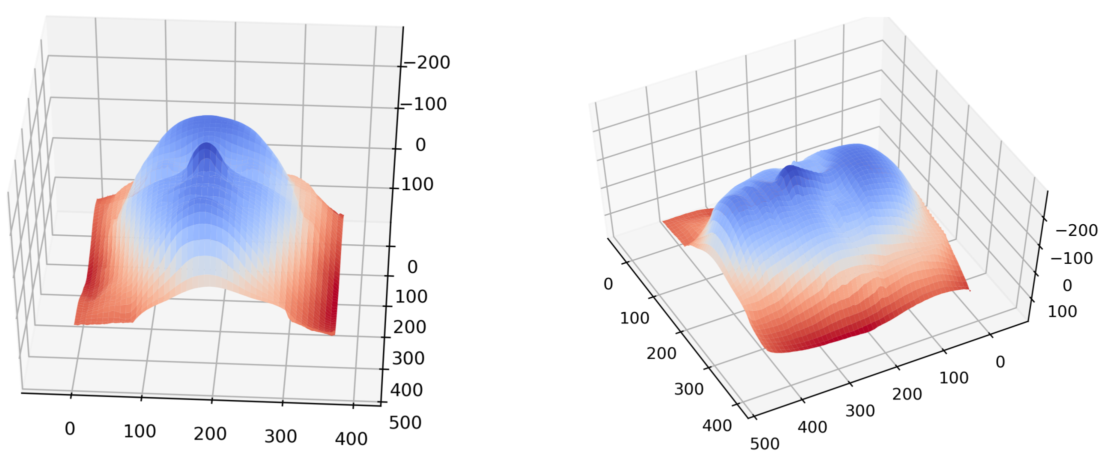

Figure 5: Depth Map from Normal

The images above resemble a shape.

2 Uncalibrated Photometric Stereo

2.1 Uncalibrated normal estimation

The matrix I can be decomposed into $\hat{B}$ and $\hat{L}$ by using the following steps:

- Performing SVD on I

$$I = U\Sigma V^T \tag{16a}$$

- Set all rows to zero in singular values matrix after first 3 rows for rank-3 approximation.

$$\Sigma = \begin{bmatrix} \sigma_1 & 0 & 0 & \dots \\ 0 & \sigma_2 & 0 & \dots \\ 0 & 0 & \sigma_3 & \dots \\ 0 & 0 & 0 & \dots \\ \vdots & \vdots & \vdots & \\ 0 & 0 & 0 & \dots \end{bmatrix} \tag{16b}$$

- The diagonal from first three rows are then extracted from the modified singular matrix ($\hat{\Sigma}$). Extract the first three rows from V^T ($\hat{V}^T$) and extract the first three columns from U ($\hat{U}$).

- Compute estimated B and L

$$\hat{B} = \sqrt{\hat{\Sigma}}\hat{V}^T \tag{16c}$$

$$\hat{L} = \hat{U}\sqrt{\hat{\Sigma}} \tag{16d}$$

2.2 Calculation and visualization

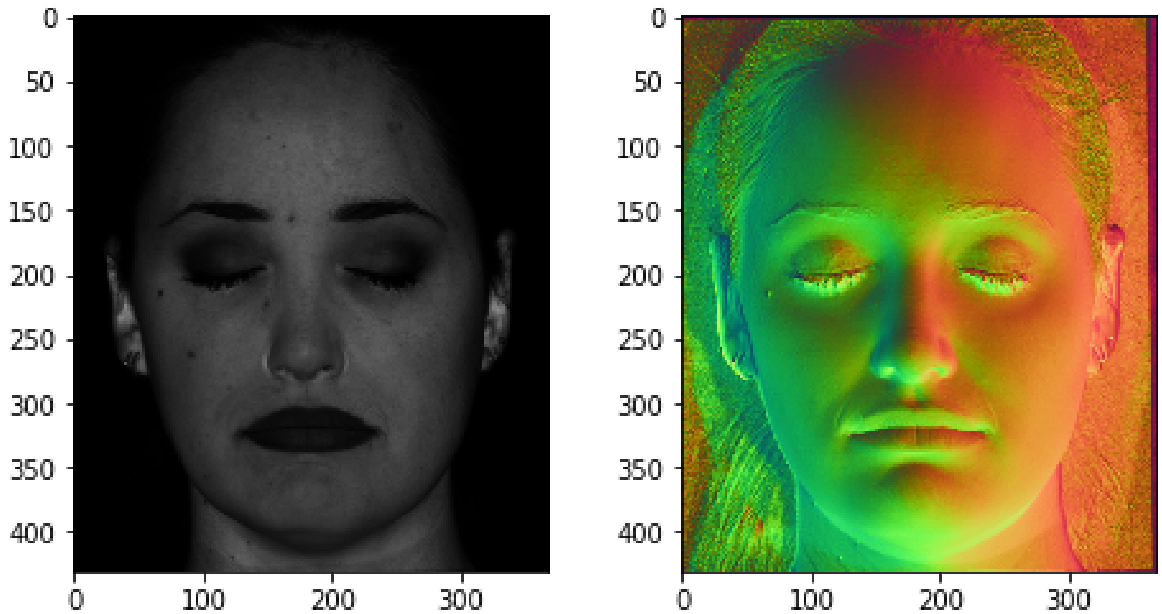

Figure 6: Visualization of albedo and normal images

2.3 Comparing to ground truth lighting

Ground truth lightning is a 3×7 matrix:

$$L_0 = \begin{bmatrix} -0.1418 & 0.1215 & -0.069 & 0.067 & -0.1627 & 0. & 0.1478 \\ -0.1804 & -0.2026 & -0.0345 & -0.0402 & 0.122 & 0.1194 & 0.1209 \\ -0.9267 & -0.9717 & -0.838 & -0.9772 & -0.979 & -0.9648 & -0.9713 \end{bmatrix}$$

The estimated lightning matrix is:

$$\hat{L} = \begin{bmatrix} -2.9926 & -3.8699 & -2.4080 & -3.7450 & -3.5913 & -3.386 & -3.3525 \\ 0.94780 & -2.3176 & 0.4994 & -0.6256 & 2.3256 & 0.4660 & -0.7928 \\ 1.8793 & 1.0146 & 0.4294 & -0.0173 & -0.3107 & -0.9127 & -1.8830 \end{bmatrix}$$

The above values indicate that the ground truth lightning, L_0 is not similar to estimated lightning $\hat{L}$. The discrepancy is a result of the 9 DOF ambiguity from the rank-k approximation of **I**. This is primarily due to the non-unique nature of the rank decomposition.

2.4 Reconstructing the shape, attempt 1

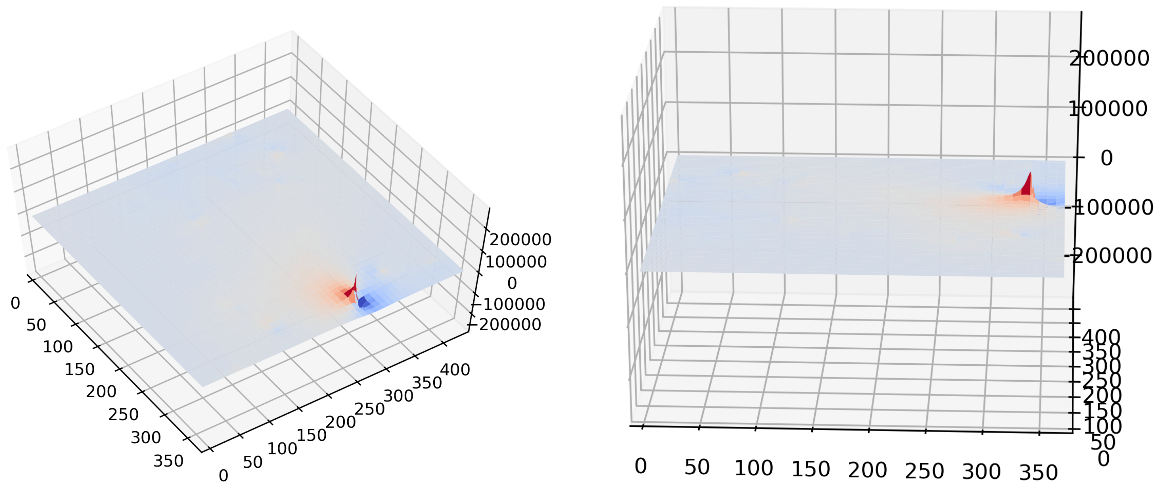

Figure 7: Depth Map from Normal

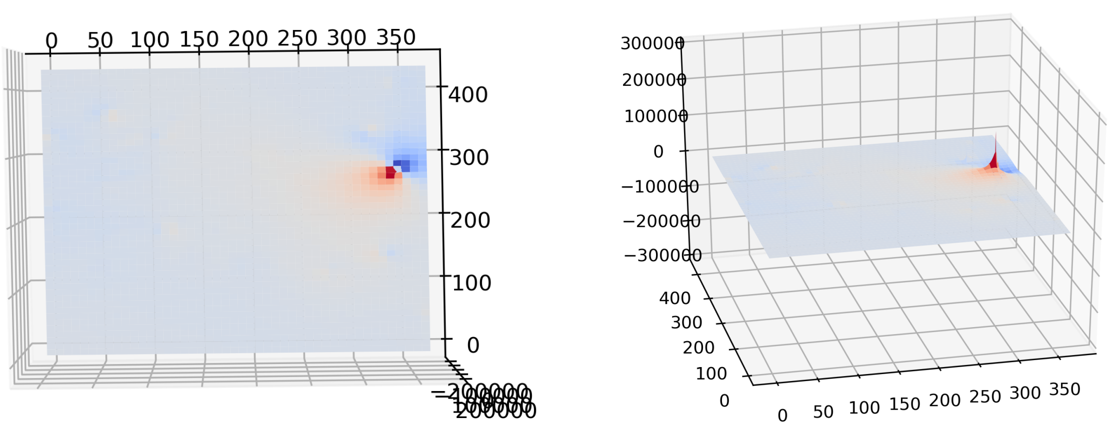

Figure 8: Depth Map from Normal

The reconstruction for this attempt does not resemble a face at all.

2.5 Reconstructing the shape, attempt 2

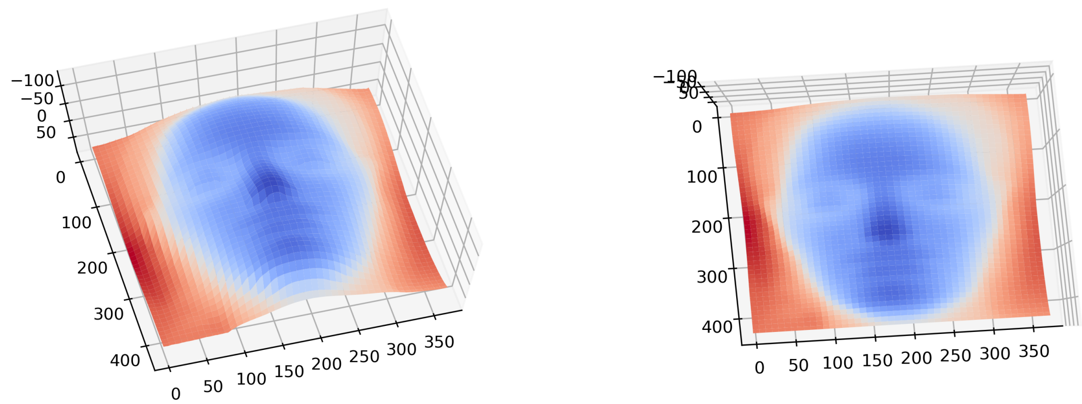

Figure 9: Depth Map from Normal

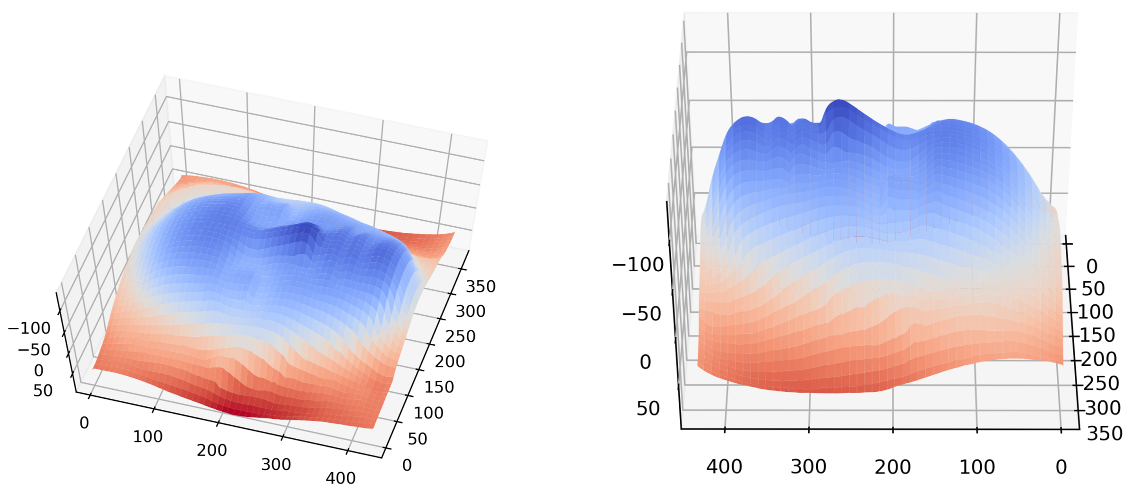

Figure 10: Depth Map from Normal

Yes, the figures above do resemble a face.

2.6 Why Low-relief?

Varying μ

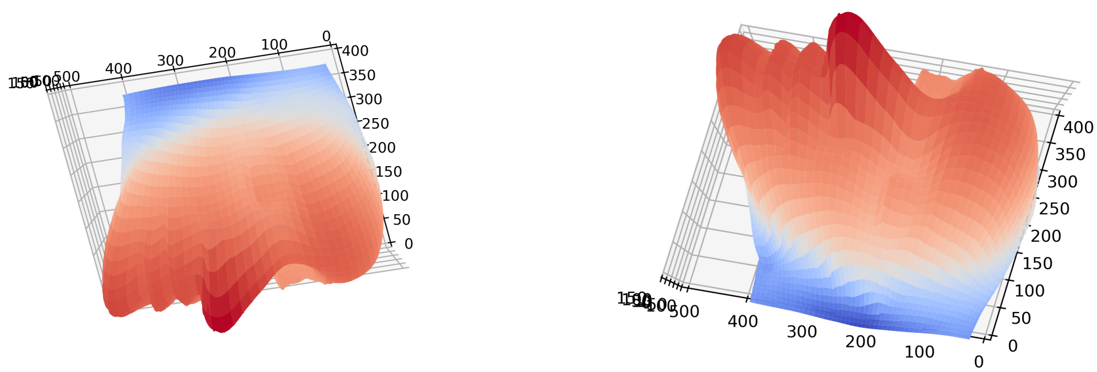

Figure 11: Varying μ

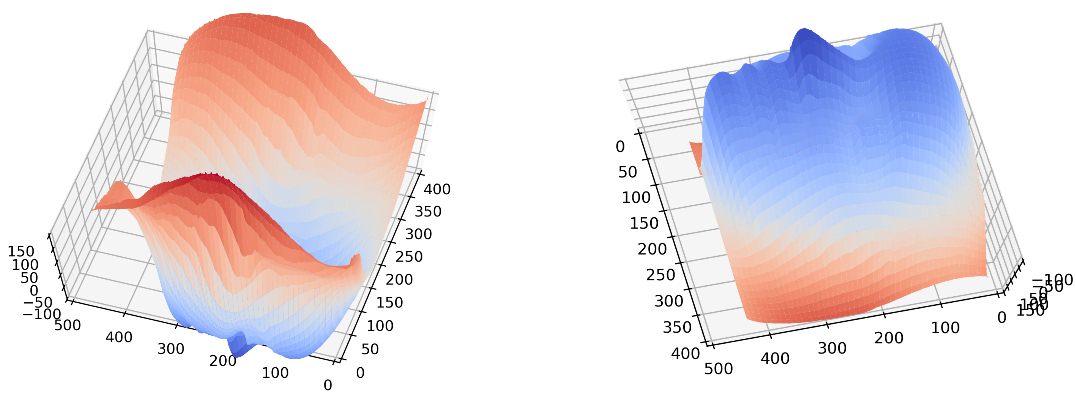

Figure 12: Varying ν

The pictures above are for $\mu = -10$ and $\mu = 5$ and $\nu = 0$ $\lambda = 0.90$. It can be noted that as μ was increased the image tilted more and also flattened. This was because the effect of x on the overall depth map was increased.

Varying ν

The pictures above are for $\nu = -1$ and $\nu = 2$ and $\mu = 0$ $\lambda = 1$. It can be noted that as ν was increased the image tilted more and also flattened. This

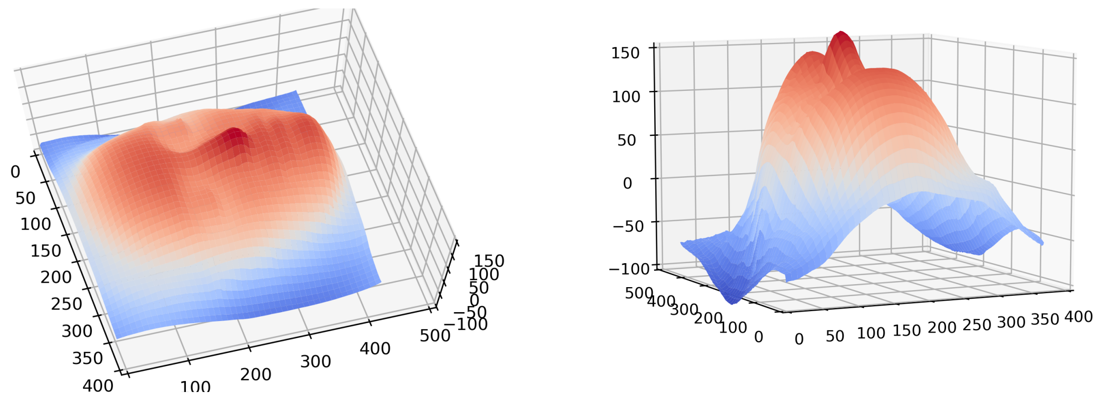

Figure 13: Varying ν

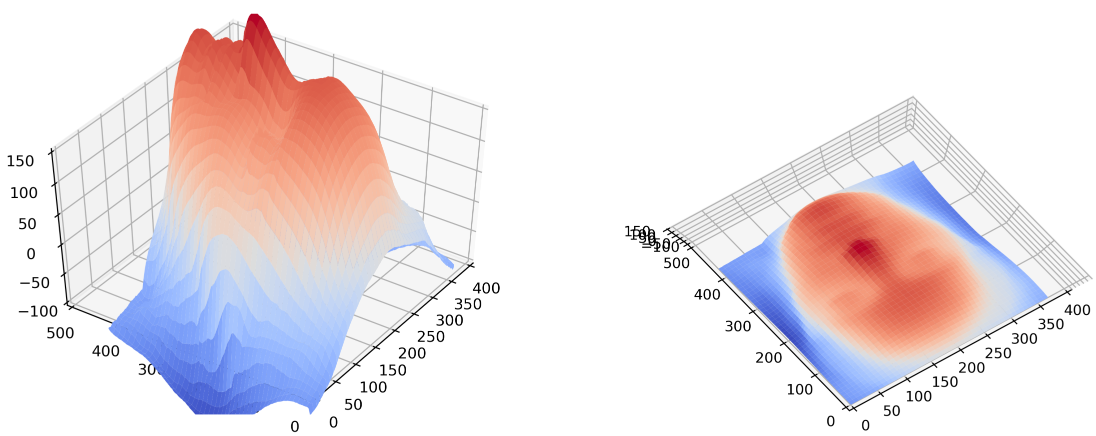

Figure 14: Varying ν

was because the effect of y on the overall depth map was increased.

Varying λ

The pictures above are for $\lambda = 0.90$ and $\lambda = 0.50$ and $\nu = \mu = 0$. It can be noted that as λ was increased the height of the image increased and flattened otherwise.

The bas-relief ambigugity are named so because the flattened forms created are extremely hard to differentiate from full reliefs when viewed from certain angles.

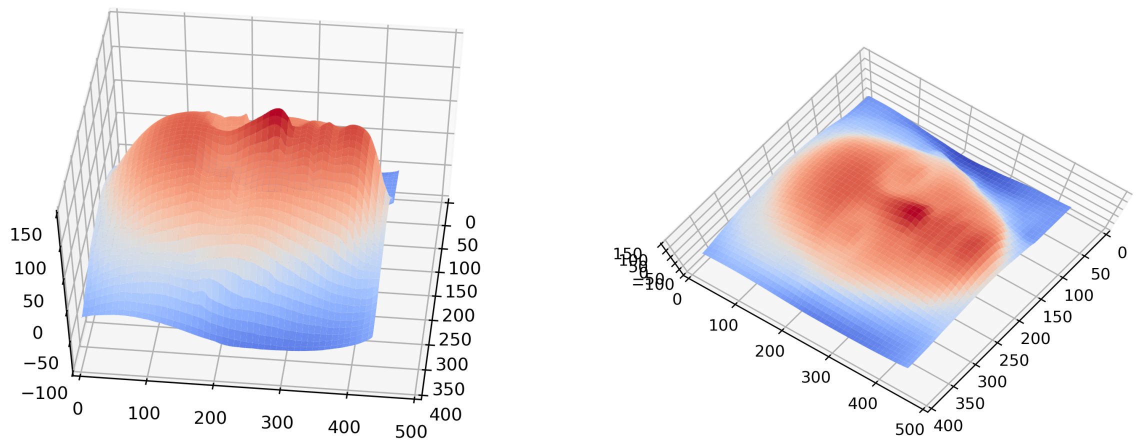

Figure 15: Varying λ

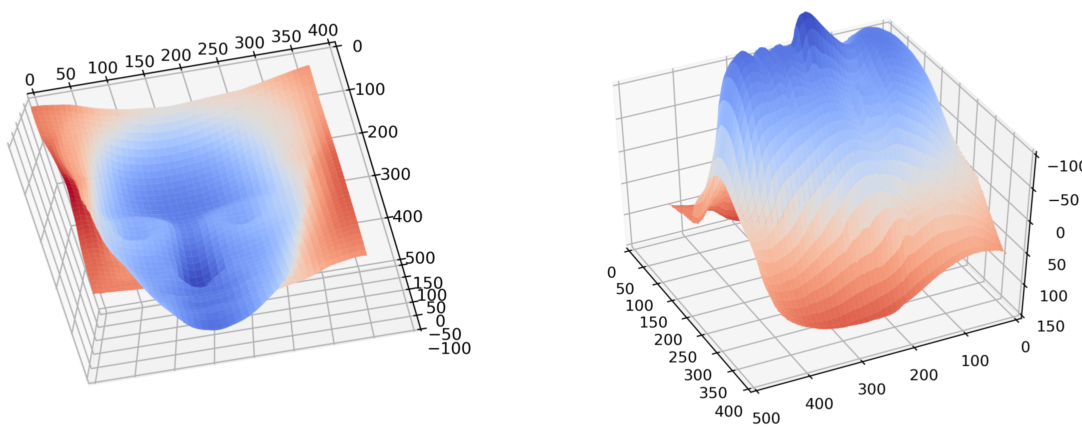

Figure 16: Varying λ

2.7 Flattest surface possible

Going by the equation for **G**, λ would need to be minimized in order to create the flattest form.

2.8 More measurements

No, acquiring more pictures will not help resolve ambiguity as the rank factorization conducted after SVD would not change.

3 Homework Feedback

3.1 Feedback

For this homeowrk, the following points were unclear:

1. For 1f it was not clear what ”expectation” meant and how to quantify it.
2. The directions of x and y were not clear for 1h.
3. The exact requirements for 2c were not obvious from the writeup.
4. The starter code was appropriate.